

General Disclaimer

One or more of the Following Statements may affect this Document

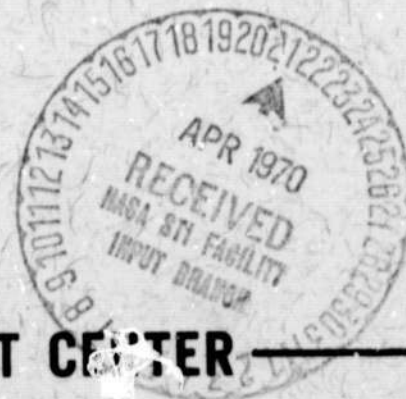
- This document has been reproduced from the best copy furnished by the organizational source. It is being released in the interest of making available as much information as possible.
- This document may contain data, which exceeds the sheet parameters. It was furnished in this condition by the organizational source and is the best copy available.
- This document may contain tone-on-tone or color graphs, charts and/or pictures, which have been reproduced in black and white.
- This document is paginated as submitted by the original source.
- Portions of this document are not fully legible due to the historical nature of some of the material. However, it is the best reproduction available from the original submission.

NASA TM X-63871

**OBSERVATIONS FROM OGO-V OF
THE THERMAL ION DENSITY AND
TEMPERATURE WITHIN THE
MAGNETOSPHERE**

**G. P. SERBU
E. J. R. MAIER**

JANUARY 1970



**GODDARD SPACE FLIGHT CENTER
GREENBELT, MARYLAND**

FACILITY FORM 602	<u> N70-24251 </u>	<u> / </u>
	(ACCESSION NUMBER)	(THRU)
	<u> 39 </u>	<u> 7 </u>
	(PAGES)	(CODE)
	<u> NASA-TMX-63871 </u>	<u> 25 </u>
	(NASA CR OR TMX OR AD NUMBER)	(CATEGORY)

OBSERVATIONS FROM OGO-V OF THE THERMAL ION DENSITY
AND TEMPERATURE WITHIN THE MAGNETOSPHERE

by

G.P. Serbu and E.J.R. Maier
Laboratory for Planetary Atmospheres
Goddard Space Flight Center
Greenbelt, Maryland

ABSTRACT

The OGO-V retarding potential analyzer experiment is operated in a voltage mode designed to yield the integral spectrum of both ions and electrons in the energy interval from 0 eV to 500 eV. Detailed results obtained with the spacecraft inside $7 R_E$ during the first 15 orbits (March - April, 1968) are presented. We can identify and group the data into three types of density profile; First, a smooth decrease in ion density from approximately 10^4 ions/cm⁻³ at $1.5 R_E$ down to the experiment threshold level of ~ 20 ions/cm³ at approximately 5 to 6 R_E . A second general type of observed density profile is typified by considerable structure within the plasmasphere and the plasmopause is identified by a factor of 3 or more drop in ion density. The third type of profile shows a density drop of a factor of 20 or more inside the $L = 7 R_E$ radial distance to values below our minimal detectable level of 20 cm^{-3} . The ion temperature observations show that within the plasmasphere the day to night temperature ratio is about

a factor of 2, with the temperature ranging from a low of 5×10^3 °K at $1.5 R_E$ on the nightside to as high as 3×10^4 °K at $3.6 R_E$ on the dayside. At the plasmopause a sudden increase in the ion temperature is observed. This increase is generally a factor of 5 or more within $0.8 R_E$, and it has been used to pinpoint the plasmopause location. Beyond the plasmopause we find a region of relatively high ion temperature, $T_i > 10^5$ °K.

INTRODUCTION

The presently accepted descriptive model of the thermal particle ($E < 10$ eV) density distribution within the magnetosphere was formulated as a result of the Whistler observations of Carpenter (1963) and Angerami and Carpenter (1966). The Whistler results have been substantiated by a variety of plasma probe observations, Gringauz (1963), Taylor et al. (1965), Binsack (1967) and recently by Harris et al. (1970) as well as observations, conducted from spacecraft, on the propagation path of ground generated V.L.F. signals (Heyborne 1966) and the study of in-situ E.L.F. noise (0.1 to 1.0 KHz) Russell et al. (1969).

In accord with these observations, the plasmasphere is the near-earth region of the magnetosphere where the thermal plasma density distribution near the equatorial plane decreases approximately with an inverse power law of the radial distance. A sharp discontinuity in the plasma density gradient occurs at the plasmopause, and beyond there exists a region of decreased density, the plasma trough. Extensive observations have been reported on the location of the plasmopause relative to the Earth, and on its radial motion which is associated with magnetic activity Carpenter (1966) Carpenter, et al. (1969) Rycroft and Thomas (1968).

In contrast to the above, observations on the thermal structure of the magnetospheric plasma at energies below tens of eV are very sparse. The electron temperature was reported by Serbu and Maier (1966) to increase as R^2 (where R is the radial distance), reaching a value of $\sim 2 \times 10^4$ °K at $5 R_E$. Gringauz (1960) deduced from Luna 1 and 2 that the ion temperature at $4 R_E$ is less than

10^4 °K. At the synchronous altitude of $6.6 R_E$, Freeman (1968) obtained ion temperatures of approximately 1.4×10^4 °K. At present no complete ion temperature measurements have been reported for the various regions of the magnetosphere.

It is the purpose of this paper to present some recent simultaneous measurements of ion density and temperature which were made in the dawn and morning quadrants of the magnetosphere.

The Experiment

A retarding potential analyzer experiment was launched on the OGO-V spacecraft to measure the density and temperature of the thermal plasma in the magnetosphere. The spacecraft was launched from Cape Kennedy on the 4th of March, 1968 at 13:06 U.T. and injected into a highly eccentric orbit at 14:02 U.T. The pertinent orbit parameters are: geocentric distance of apogee 146,751 km, initial perigee height of 337 km (during the first six orbits the perigee height increased to 557 km) and a period of 62 hours. The sun - earth - satellite angle at the first apogee was 35° . This observatory was inserted into orbit with three axis stabilization; subsequently, optimum orientation of experiments along with flawless spacecraft systems operation was achieved. To the present, 18 months of continuous data have been obtained with no noticeable degradation in operation of the experiment.

The OGO-V retarding potential analyzer experiment is operated

in a voltage mode designed to yield the integral spectrum of both ions and electrons in the energy interval from 0 eV to 500 eV. The principle of operation of this experiment has been discussed previously and the interested reader is referred to the literature: Bourdeau, et al. (1961); Serbu (1965); Whipple and Parker (1969).

Table 1 contains a schematic representation of the sensor grid arrangement, along with an abbreviated wave-shape diagram to illustrate the voltage program used for measuring the ion spectrum. Similar wave-forms but with reversed voltage polarity are used for the electron mode of operation. The sensor is a planar circular cup, 7 cm in diameter, inside of which are contained four parallel grids which are spaced 4 mm apart. The large diameter to depth ratio for this sensor serves to minimize stray currents due to secondary emission from the walls of the sensor, and in addition this geometry better defines the solid angle for collection of the particle flux. The sensor aperture area is 3 cm^2 ; while the collector subtends a 160° angle. As can be seen in the top line of Table 1, a square wave of -14 volts is applied to the aperture during the ion mode of operation. The aperture voltage plus the spacecraft-to-plasma potential (assumed to be zero in this discussion) serves to exclude all electrons whose energies are less than the aperture potential, 14 eV in this example. The wave-form applied to the retarding grid is a linearly decreasing staircase voltage ranging from +15 to -5 volts. During this voltage sweep, 32 current measurements are made at approximately

0.5 volt intervals. This sweep is followed by one whose potential varies from +500 to 0 volts. During the later sweep nine current measurements are made at intervals of approximately 40 volts and 7 current measurements at 20 volt increments.

In Table 1 it can be seen that the suppressor grid voltage is always more negative than the collector voltage, thereby reducing the secondary electron current from the collector. The current as a function of sweep voltage is measured in two linear ranges by a bi-polar electrometer sensitive in the range from 10^{-12} to 10^{-7} amperes. Sufficient dynamic range and spatial resolution are available with this experiment to yield continuous data on the thermal plasma density and temperature from above the ionosphere out to the plasmopause.

The time required to complete the ion sweep is dependent upon the spacecraft telemetry sampling rate. At the slow rate of 1 kilobit/sec, the required time is 18 seconds, and at the 8 and 64 kilobit/sec rate the time required is 2.25 seconds. A complete set of data consisting of ion and electron mode sweeps in each of the two electrometer ranges thus requires 4 of these basic time units.

The experiment is mounted on the OGO-V orbital plane experiment platform (OPEP-2) which aligns the experiment sensor in the orbital plane. Thus, the angle to the velocity will be zero at apogee and perigee. Superimposed on the OPEP

orientation is a $\pm 120^\circ$ scan mechanism which can be commanded from the ground to assume any preferred direction in a plane perpendicular to the spacecraft orbital plane and to the spacecraft-Earth vector. An alternate mode of operation is to scan through a 240° angle in that plane at the rate of 3° per second. With this mounting arrangement the R.P.A. experiment can obtain an integral spectrum at nearly all angles with respect to the velocity vector; thus, effects due to streaming of plasma relative to the sensor can be studied in detail.

Data Analysis

Interpretation of the current-voltage (I-V) response characteristic to yield parameters descriptive of the ambient medium is accomplished by comparing the data to theoretical response functions. The response function appropriate for the case of a planar retarding analyzer operating in a medium where the spacecraft potential, V_S , is small and where the spacecraft may have a velocity comparable to ion thermal velocities has been treated by Whipple (1959). He obtained the following expression for the ion current as a function of retarding potential V_R :

$$I_+ = \alpha N_e A v \cos \theta \left\{ 1/2 + 1/2 \operatorname{erf} (x) + \frac{a \exp (-x^2)}{2 \sqrt{\pi} v \cos \theta} \right\}$$

where:

$v \cos \theta$ is the component of spacecraft velocity parallel to the sensor axis

α is the grid transparency

N is the ambient ion concentration

A is the area of the retarding analyzer aperture

$$a = \sqrt{2 kT/m}$$

T = ambient ion temperature

$$x = (v \cos \theta - \sqrt{2 eV_R/m})/a$$

and k , m , e are, respectively, Boltzmann's constant and the proton mass and charge. Note that this function was derived for retarding values of V_R , i.e., the retarding potential was more positive than the ambient plasma.

If V_R is negative with respect to the plasma, the probe is said to be in the accelerating region of its response function. For the ideal planar probe, the current detected in the accelerating region is expected to be independent of the value of the potential. This ideal characteristic will be obtained only in the limit of true planar geometry, viz., a probe whose external surfaces are at plasma potential operating in a plasma having a Debye length less than the dimensions of the sensor. For larger values of the Debye length, and for particle velocities greater than the spacecraft velocity, it is expected that the response characteristic in the accelerating region of applied potentials will exhibit a smooth transition to the response characteristics of a spherical probe:

$$I = aNe A \{1 + eV_R/kT\}/2 \sqrt{\pi}$$

No exact solution has been obtained for the characteristic in the accelerating region of a moving finite probe with nonzero potential. Whipple and Parker (1969) have derived the response function for electrons for the case of a slowly moving spacecraft. The essential point of their work which bears on the interpretation of the present ion data is that the net charge on the spacecraft can impose a limit on which of the particle trajectories can be sampled by the retarding analyzer. More specifically, if the spacecraft charge is repulsive with respect to the species of particles to be sampled, the incident particles will encounter a repulsive potential barrier along their trajectories toward the sensor. The magnitude of the barrier is determined by the geometry of the spacecraft, the values of exposed potentials on solar panels, etc., and the ambient plasma and radiation properties; it may be a significant fraction of the spacecraft potential. Thus, in the low density region of the plasmasphere where the spacecraft is expected to have slightly positive potentials, the "true" response characteristic may not be observed for values of sweep voltage near zero retardation or accelerating with respect to the plasma. That is, the transition from planar probe characteristic to spherical probe characteristic will not occur. Thus, we have fitted the observed current voltage data to:

$$I = I_+ (V_R) + B$$

for values of $V_R = (V \text{ sweep} - V_S) > 0$ and to $I = I_+ (0) + B$ for values of $V_R = (V \text{ sweep} - V_S) \leq 0$ where I_+ is the expression given

in equation (1), and B is a possible constant background flux of energetic particles which are unaffected by V_R . The iterative procedure yields the best estimation of the values for the ion density N, the ion temperature V, the background flux B, and the spacecraft potential V_S .

As stated in a previous section, a complete ion mode consists of 96 observations of the flux obtained in about 9 seconds. Instead of fitting a single set of observations to the theoretical function, groups of data from two successive modes were treated as one set of observations. Thus, when the spacecraft data system was in the 8 or 64 kilobit/sec telemetry mode, a set of best estimates for N, T, V_S , and B could be obtained every 18 seconds.

Comparisons of the results obtained for successive analyses did not show any significant dependence of the values of the temperature (T) and density (N) on the orientation of the sensor as it scanned the forward direction. The main body of the results obtained from this type of analysis is given in the later section entitled Experimental Results. We now discuss an alternate procedure for obtaining the values of the ambient ion density and temperature.

The motion of the spacecraft through the ambient medium results in ions incident on the sensor at a velocity which is the vector sum of the (negative of the) spacecraft velocity, any ion bulk flow velocity, and the ion thermal velocity. From the data obtained during a complete scan of the OPEP (approximately a two minute interval), the subset of points obtained when the retarding potential was near zero has been selected. Figure 1 shows the

currents observed as a function of angle for the times during the April 4th inbound pass of the spacecraft. The open circle data points were obtained when the spacecraft was near $1.8 R_E$ geocentric distance. They show a factor of three variation of ion flux with angle to the velocity vector. The darkened circle data points were obtained when the spacecraft was at $4.2 R_E$; they show an essentially isotropic distribution of flow. From these observations of the angular distribution of the ion flow in the spacecraft coordinate system we conclude that:

1) at $4.2 R_E$ the ion thermal speed must be greater than the spacecraft velocity.

2) at $1.8 R_E$ the ion thermal speed must be less than the spacecraft velocity. The solid lines in Figure 1 show the variations of flux expected on the basis of the actual spacecraft velocity and the two ion temperatures indicated. These two temperatures have been obtained by the more extensive retardation analysis discussed earlier and are typical of the regions cited in this example. The agreement of the observed and predicted flows confirms the values of the temperature obtained from the retardation analysis. Gringauz et. al. (1967) have used essentially this dependence of the ion flux on sensor aspect angle to estimate the ion temperature in the altitude range 4000-8000 km. They observed the variation of the ion flux as Elektron 2 rotated and thus obtained an upper limit of $10,000^{\circ}$ for the ion temperature under the assumption that the maximum and minimum fluxes were observed, respectively, parallel and anti-parallel to the spacecraft velocity vector.

Experimental Results

In Figure 2 are plotted the ion density profiles obtained for the first 15 orbits of OGO-V. The dates of the perigee passes are shown in the middle of the figure. Inbound, or day-time, traversals from $L = 7$ to $L = 1.5$ are shown in the left panel of the figure, and the outbound, night-side, densities are plotted in the righthand panel. A series of tick marks along the ordinate serve to define the 10 ions/cm^{-3} level for each curve; successive curves are spaced two orders of magnitude apart in the vertical direction. The ordinate scale is shown in the lower left corner of each panel.

We can identify and group the data into three types of density profile: First, a smooth decrease in ion density from approximately 10^4 ions/cm^3 at $1.5 R_E$ down to the threshold level of $\sim 20 \text{ ions/cm}^3$ at approximately 5 to 6 R_E . The March 7th and 9th profiles are typical of these smoothly decreasing profiles; generally they are associated with very low K_p values. The plasmopause location for these quiet time orbits cannot be identified; presumably it is located outside 7 R_E . A second general type of observed density profile is typified by the passes of March 30, and April 2nd and 4th. During the times of these profiles considerable structure is noted within the plasmasphere, and the plasmopause is identified by a factor of 3 or more drop in ion density. The third type of profile is illustrated by the data inbound on the 17th and outbound on the 30th of March.

In these, the density drops a factor of 20 or more inside of $L = 7 R_E$ radial distance to values below our minimum detectable level of 20 cm^{-3} .

In Figure 3 are plotted the ion temperature profiles obtained concurrently with the density data of Figure 2; the same plotting format is used. The tick marks are placed at the $10^5 \text{ }^\circ\text{K}$ level for each curve; successive curves are spaced two orders of magnitude along the ordinate.

A detailed discussion of the temperature profiles is deferred to a subsequent figure; this data presentation illustrates the general features and variability of the plasmasphere temperature profiles as observed over an extended period of time.

In general, the proton temperature increases smoothly from a level near $10^4 \text{ }^\circ\text{K}$ at $2 R_E$ up to a few times $10^4 \text{ }^\circ\text{K}$ at 3 to $4 R_E$. Values in excess of $10^5 \text{ }^\circ\text{K}$ are observed, primarily at large radial distances. Occasionally local temperature enhancements to this level are observed inside $3.5 R_E$; e.g., the outbound passes of March 12th and 17th show a temperature enhancement of about a factor of ten near $3 R_E$. The combined data of Figure 2 and 3 indicate that the energy density of the thermal particles in the plasmasphere lies in the range from 10^{-8} to $10^{-10} \text{ ergs/cm}^3$.

DISCUSSION OF RESULTS

Figure 4 is a more detailed presentation of the ion temperature measurements obtained during the perigee pass of March 14, 1969. The L-values for the inbound and outbound trajectories are shown on the lower two abscissas in the figure. The perigee for this revolution occurred at 23:46 U.T. on the 14th of March, 1968 and was located above the Pacific Ocean (-29.7° latitude; -92.5° longitude) at an altitude of 476 km.

The data of this figure begin at 22:07 U.T. with the spacecraft at $5 R_E$ on the inbound trajectory, and end nearly 3.5 hours later at 01:23 U.T. on the 15th of March, 1968 at which time the spacecraft is outbound at $5 R_E$. Data obtained within ± 15 minutes of perigee time have not been reduced due to the high negative potential of the spacecraft and the variation of ion constituents as a function of altitude below $1.5 R_E$. The plotted values of ion temperature were calculated using a single ion constituent (H^+) to represent data obtained throughout the protonosphere. This assumption agrees with results obtained by the mass spectrometer observations of Taylor et al. on OGO III (op. cit.) and Harris et al. on OGO-V (1969).

The inbound trajectory for this orbit is located on the dayside of Earth; at $4 R_E$ the subsatellite point was at local noon. The trajectory intersects the equatorial plane near $5 R_E$ and is southbound. The middle abscissa in the figure pertains to the inbound trajectory and shows the L value and geographic latitude for each radial distance. The inbound data, the solid

line, between L of 5 and 4.2 show the ion temperature to be near 10^5 °K with large variations about a uniform structure. At L = 4.2 a large decrease in the ion temperature suddenly occurs; within less than $0.1 R_E$ the temperature drops by a factor of 5. The jump in the temperature profile occurs at the same time at which the density increases by a factor of 10. We observe that at the plasmopause a significant change in the ion temperature profile is present. A similar ion temperature jump occurs with the spacecraft outbound at L = 3.6; within $0.1 R_E$ the temperature increases from 16,000 °K to 190,000 °K at the time the density decreased by a factor of 50. These observations appear to be consistent with the magnetospheric convection theories of Axford and Hines (1961); Nishida (1966); and Brice (1967) which identify the plasmopause as the boundary between the plasmasphere and the hot magnetosphere plasma which is in convective flow up the geomagnetic tail. Freeman and coworkers (1967) have observed convective flow of ions of energy less than 50 eV with the ATS-1 synchronous orbit satellite at $6.6 R_E$. Recently Banks and Holzer (1969) have predicted that 10 eV ions ($\sim 10^5$ °K) will be found in the magnetotail as a consequence of plasma escape via the polar wind.

As the spacecraft descends into the plasmasphere the ion temperature decreases from 55,000 °K at $4 R_E$ to a value of 14,000 °K at $1.5 R_E$. cursory examination of data below $1.5 R_E$ indicates that the temperature continues to decrease to values of the order of 10^3 °K at altitudes near perigee. From the temperature difference between $4 R_E$ and $1.5 R_E$ we calculate a temperature

gradient along the radius vector of 2.5°K/Km . We can also compute a temperature gradient along the field line assuming the 1000 km level as the base of the field line, with an average value of 3000°K for the temperature at this level. With this assumption at $L = 4$ the temperature gradient along the field line is 0.9°K/Km , and at $L = 3, 2$ and 1.5 it is 1.3°K/Km , 1.1°K/Km , and 1.5°K/Km , respectively. These values for the thermal gradients along the field line are in fair agreement with the protonosphere value of $\frac{\Delta T_1}{\Delta R} < 1^{\circ}\text{K/Km}$, as determined from Explorer 22 by Brace, Reddy and Mayr (1967) at the 1000 km altitude, and the Millstone Hill radar observations of Evans (1967).

Outbound from perigee the spacecraft is above 20° North latitude, on the night side of Earth. At $3 R_E$ outbound the subsatellite point occurs at 0300 hrs. local time. The lower horizontal scale of Figure 4 shows the appropriate L shell and geographic latitude pertaining to the outbound ion temperature data, dashed curve. Within the plasmasphere, which on the night side on this day extended out to $L = 3.6 R_E$, the ion temperature profile closely parallels the dayside temperature profile. However, the temperature values are lower in magnitude by a factor of 2. Brace (1969) has shown that at the 1000 km level, in the latitude interval -20° to $+20^{\circ}$, the day to night electron temperature ratio varied by a factor ranging from 2 to 2.8, over a three year consecutive period of observation. The observed plasmasphere day to night ion temperature ratio is indicative of the strong field line coupling between the plasmasphere and the 1000 km level of the ionosphere. The computed

temperature gradients along the field line for the night side are 0.4, 0.3, 0.4 and 0.5 °K/Km for the L shells 1.5, 2.0, 3.0 and 4.0 respectively.

The plasmasphere temperature profile undergoes marked changes in structure from one orbit to the next; these changes appear to be temporal and they show a high correlation with the magnetic activity index, K_p . Data from three orbits during which the daily sum of the magnetic index ΣK_p was from 8 to 11 are grouped in figure 5a, and data from three orbits for which ΣK_p was from 19+ to 27- are grouped in Figure 5b. During times of low K_p the temperature profile is relatively smooth and uniformly increasing with radial distance; some structure is apparent only beyond $L = 4$. The plasmopause is identifiable in only one of these quiet profiles; the vertical dashed line locates the plasmopause for the outbound trajectory of March 9. For days during which $\Sigma K_p > 19$, the plasmasphere temperature profiles show marked spatial variations about the mean gradient and generally the plasmopause position is readily located on the basis of a factor of 10 or more increase in temperature within a fraction of an Earth radius. Inside the plasmasphere during time relatively high magnetic activity, $\Sigma K_p > 15$, localized regions of enhanced ion temperatures are observed generally in the vicinity of $L = 3$. As can be seen in figure 5b, near $L = 3$ we observe that within $0.5 R_E$ the ion temperature increases smoothly by a factor of three or more and then smoothly decreases to nearly the previous level. In a majority of these instances

the observations can be viewed in terms of either a spatial or temporal increase in the measured energy of the thermal plasmasphere ions. In Table 2 we summarize the data used for identifying the plasmopause location and magnitudes of changes observed in the density and the temperature. Dayside data refers to inbound trajectories, and night side to outbound; the time of perigee is given in column 2. The average value of K_p for three hours before and after the perigee time is listed in column 3. The value N_i/N_o refers to the measured ratio of ion density inside the plasmasphere (N_i) to the ion density outside (N_o). The ratio T_o/T_i is a measure of the temperature jump at the plasmopause. As can be seen in the table the three classes of density profiles discussed above are closely associated with the three-hour K_p centered about the perigee time. In general we note that a large drop in density at the plasmopause is accompanied by a large increase in temperature. The temperature ratios observed at the plasmopause on the night side of earth are larger than the ratios for the dayside. This effect is due to the fact that night side ion temperatures inside the plasmasphere are lower by a factor of 2 than the dayside values, whereas, beyond the plasmopause the temperature is essentially uniform throughout the time sector.

We have used a plasma density decrease of at least a factor of 3 to define the existence of the plasmopause. The position of the innermost such decrease has been plotted vs the 3 hourly average K_p for the corresponding time. These data are shown in Figure 6. Here we have also shown other observations of the

plasmopause - K_p relationship. Included are data obtained from Whistler observations by Carpenter (1966) and data obtained from direct measurements by Bezrukikh (1968), Binsack (op. cit.), and Taylor et al. (1966). The OGO-V results are shown as the solid data point with the solid line representing the least square fit. All these measurements are in good agreement regarding the variation of plasmopause position with K_p . The change in the radial distances of the plasmopause is proportional to $K_p \times 0.5$. Our observations show the boundary about $1 R_E$ earthward of earlier observations. This is attributed both to the increased solar activity in 1968 and to the fact that in the plotted data OGO-V has not sampled the evening quadrant of the plasmasphere where Carpenter has shown a bulge to occur.

The plasmopause location identified on the basis of the ratio T_o/T_i (see Table 2) is shown in Figure 7. The heavy solid line indicates the average location of the plasmopause as observed by Carpenter. Superimposed on this figure we have located the plasmopause position, the solid square points, based on our observations of a steep thermal gradient in the measured ion temperature. A generally good agreement between the thermal gradient data and the Whistler average quiet time plasmopause location is noted.

CONCLUSIONS:

The ion temperature observations show that within the plasmasphere the day to night temperature ratio is about a factor of 2, with the temperature ranging from a low of 5×10^3 °K at

1.5 R_E on the nightside to as high as 3×10^4 °K at 3.6 R_E on the dayside. The average thermal gradient along the field line on the dayside is typically $\Delta T/\Delta R \approx 1.2$ °K/Km and on the nightside $\Delta T/\Delta R \approx 0.4$ °K/Km. At the plasmopause a sudden increase in the ion temperature is observed. This increase is generally a factor of 5 or more, within 0.8 R_E and it has been used to pinpoint the plasmopause location as shown in Figure 7. Beyond the plasmopause we find a region of relatively high ion temperature, $T_i \geq 10^5$ °K.

We have presented some preliminary results on ion temperature profiles as measured for the first time in the outer protonosphere. These observations of the relatively high density, at the outer boundary of the plasmasphere, of about 100 ions/cm³ at 4 R_E and an apparent temperature of a few times 10^4 °K are not consistent with a simple diffusive equilibrium distribution along a closed magnetic field line. We propose that the majority of these particles are protons 'trapped' for a time of the order of one day during which they traverse the length of the field line tens of times. Because of the relatively small gyro-radius of these particles it is unlikely that they have crossed field lines from an outer boundary in order to populate the inner L-shells. The most likely source seems to be the traditional "isothermal" ion-exosphere which would populate the L = 3 shell with tens of ions/cm³ at 3000 °K. We note that ions flowing upward from below 1.5 R_E on the L = 3 shell will have a pitch angle of less than 60° at 1.8 R_E . Thus, Coulomb scattering above that height is more likely to result in trapping than in

loss. This process can lead to a population of thermal particles trapped at high altitudes. The self-collision life time of 0.5 eV particles in a plasma of density 100 ions/cm^3 is 2400 seconds (Spitzer, 1965; Trubnikov, 1965); thus, the majority of the ionospheric particles with a Maxwellian velocity distribution will be lost rapidly. However, the self-collision time for 5 eV particles in a plasma of density 100 ions/cm^3 is 8×10^4 seconds. The computed bounce periods for the 0.5 eV and the 5 eV particles are 3000 seconds and 1000 seconds. Thus the 5 eV particles will survive 40 or more bounces, whereas, the 0.5 eV particles will be Coulomb scattered into the loss cone in one bounce period. The discrimination of this process against low energy particles is suggested as an explanation of the apparent high temperature of the ions. If the tail of the Maxwellian distribution of ionospheric particles is the source for these suprathermal protons then their number density would decrease rapidly at increasing energy. Thus the maximum number of particles would be found at the minimum energy required for the particle to have a significant trapping life time. Alternately, wave interactions with the thermal protons in the plasmasphere may result in energization and slight deflections of the protons as they pass through the interaction region. Particles so trapped would have lifetimes as discussed earlier.

Finally, thermal contact between these ions and the ambient electrons is estimated to result in an energy transfer to the

electrons comparable to that from ionospheric photoelectrons flowing along closed field tubes. Thus, as with photoelectrons, the observed ions are an energy reservoir for the ionosphere which is neither dominant nor negligible; their influence will require considerably more detailed study.

ACKNOWLEDGEMENTS

We gratefully acknowledge the contributions of G. Barnard, E. Zellner and R. Lott who designed and tested the experiment package. We also wish to thank S. Coe and H. Sagges who were responsible for the computer programming.

LIST OF FIGURES

- Table 1 - Schematic representation of the OGO-V Retarding Potential Analyzer, showing the Sensor grid arrangement and an abbreviated wave-form diagram. All voltages are referenced to spacecraft ground.
- Table 2 - Tabulation of data used in identifying the location of the plasmopause. The identification is made on the basis of either a jump in the temperature ratio (T_o/T_i) or a jump in the density ratio (N_i/N_o). The dashed lines indicate that identification could not be made on the basis of the data obtained inside $L = 7 R_E$.
- Figure 1 - The data points represent the ion current collected at zero retardation voltage as a function of the angle between the sensor normal and the velocity vector. The smooth curves plotted are the probe response function evaluated as a function of angle for the temperatures indicated. These temperatures were obtained from the computer fits to the complete retardation characteristic (sweep range +15 to -5 volts).
- Figure 2 - Observations of Ion Density in the magnetosphere for the first 15 consecutive orbits of OGO-V. The scale shown at the lower left corner slides along the ordinate to the indicated 10^3 level of each curve. The date of perigee is shown in the center, time sequence is from left to right.
- Figure 3 - Observations of Ion temperatures in the magnetosphere for the first 15 consecutive orbits of OGO-V. The scale shown at the lower left corner slides along the

ordinate to the indicated 10^5 level of each curve.

Figure 4 - Detailed temperature profile for the 14th March, 1968 orbital pass. The abscissa is given in terms of Earth radii (R_E) and the L-shell parameters for both inbound and outbound portions of the orbit. The data begins as the spacecraft crosses the geographic equator inbound near $5 R_E$ and terminates some 3 hours later when the spacecraft is outbound at 32° north latitude.

Figure 5 - A series of ion temperature profiles grouped on the basis of the 3 hourly magnetic activity index K_p . The top panel (a) shows the measured profiles for relatively "quiet" times and the lower panel (b) for "disturbed" periods.

Figure 6 - Data showing the observed radial distance of the plasmopause as a function of the K_p value. A comparison of data obtained over a 5 year period from six spacecrafts is also shown.

Figure 7 - Projection on the equatorial plane of the plasmopause, as identified on the basis of a thermal discontinuity. The average values of ion temperatures are also indicated. The heavy solid line indicates the average location of the plasmopause as observed by Whistlers.

REFERENCES

- Angerami, J.J., and D.L. Carpenter, Whistler studies of the plasmopause in the magnetosphere, 2, electron density and total tube electron content near the knee in magnetospheric ionization, *J. Geophys. Res.*, 71, 711, 1966.
- Axford, W.I., and C.O. Hines, A unifying theory of high-latitude geophysical phenomena and geomagnetic storms, *Can. J. Phys.*, 39, 1433-1464, 1961.
- Banks, P.M., and T.E. Holtzer, High-Latitude Plasma Transport: The Polar-Wind, *J. Geophys. Res.*, 74, 6317-6331, 1969.
- Bourdeau, R.E., J.E. Jackson, J.A. Kane, and G.P. Serbu, Ionospheric Measurements using environmental sampling techniques, *Proc. COSPAR Symposium*, North Holland Publishing Co., Amsterdam, 1961.
- Bezrukikh, V.V., Results of Measurements on the density of charged particles in the Earth's plasma envelope carried out from satellites Electron 2 and Electron 4. Paper presented at The International Symposium on the Physics of the Magnetosphere, Washington, D.C., 1968.
- Binsack, J.H., Plasmopause observations with the MIT experiment on IMP 2, *J. Geophys. Res.*, 72, 5231, 1967.
- Brace, L.H., B. M. Reddy, and H.G. Mayr, Global behavior of the ionosphere at 1000 km altitude, *J. Geophys. Res.*, 72, 265, 1967.
- Brace, L.H., The Global Structure of Ionosphere Temperature, Paper A.1.5. presented at 12th Planetary Meeting of COSPAR, May, 1969; also Goddard Space Flight Center document X-615-69-158.

- Brice, N.M., Bulk motion of the magnetosphere, J. Geophys. Res., 72, 5193-5211, 1967.
- Carpenter, D.L., Whistler evidence of a "knee" in the magnetospheric ionization density profile, J. Geophys. Res., 68, 1675, 1963.
- Carpenter, D.L., Whistler studies of the plasmapause in the magnetosphere, 1, temporal variations in the position of the knee and some evidence on plasma motions near the knee, J. Geophys. Res., 71, 693, 1966.
- Carpenter, D.L., C.G. Park, H.A. Taylor, and H.C. Brinton, Multi-Experiment Detection of the Plasmapause from EOGO Satellites and Antarctic Ground Stations, J. Geophys. Res., 74, 837, 1969.
- Evans, J.V., The heating of the protonosphere, Space Research VIII - North Holland Publishing Co., Amsterdam, P. 717-728, 1967.
- Freeman, J.W., Jr., Observation of flow of low-energy ions at synchronous altitude and implications for magnetospheric convection, J. Geophys. Res., 73, 4151, 1968.
- Freeman, J.W., Jr., C.S. Warren, and J.J. Maguire, Plasma flow directions at the magnetopause on January 13 and 14, 1967, J. Geophys. Res., 73, 5719, 1968.
- Freeman, J.W., Jr., and J.J. Maguire, Gross local-time-particle asymmetries at the synchronous orbit altitude, J. Geophys. Res., 72, 5257, 1967.

- Gringauz, K.I., V.V. Bezrukikh, V.D. Ozerov, and R. Ye. Rybchinsky,
A study of interplanetary ionized gas, energetic electrons,
and corpuscular solar emission, using three-electrode charged-
particle traps set up on the second Soviet cosmic rocket
LUNA 2, DOKL, AKAD, NAUK USSR, 131, 1301-1304, 1960 a.
- Gringauz, K.I., S.M. Balandina, G.A. Bordovskii, and N.M. Shyutte,
On the results of tests with three-electrode charged particle
traps in the second radiation belt and in the outermost
belt of charged particles, Space Res., 3, 432-437, 1963.
- Gringauz, K.I., V.V. Bezrukikh, T.K. Breus, Method of Deter-
mination of Ion Temperature by the Variations of Satellite -
Induced Ion Trap Currents and Estimate of the Upper Limit
of Ion Temperature at Altitudes of 10,000 Kilometers and Higher
According to Data of AES "Elektron-2". Kasmicheskiye ISSLE-
DOVANIYA TOM 5, VYPUSK 2, 245-250, IZDATEL'STVO "NAUKA", 1967.
- Harris, K.K., G.W. Sharp, The structure of the topside ionosphere
from early orbits of OGO-V, Space Research X, North-Holland
Publishing Co., Amsterdam, 1969.
- Harris, K.K., G.W. Sharp, C.R. Chappell, Observations of the
plasmopause from OGO-V, J. Geophys. Res., 75, 219, 1970.
- Heborne, R.L., Observations of Whistler mode signals in the OGO
Satellites from VLF ground station transmitters, Ph.D.
thesis, SEL-66-094 Radio science Lab., Stanford University,
Stanford, Calif., November, 1966.
- Ludwig, G.H., The Orbiting Geophysical Observatories, Space
Technology Vol. II, Publications of Goddard Space Flight
Center 1963, U.S. Government Printing Office, Washington,
D.C., 1963.

- Nishida, A., Formation of a plasmopause, or magnetospheric plasma knee, by combined action of magnetospheric convection and plasma escape from the tail, *J. Geophys. Res.*, 71, 5669-5679, 1966.
- Russel, C.T., R.E. Holzer, and E.J. Smith, OGO-3 observations of ELF noise in the magnetosphere 1. Spatial extent and frequency of occurrence, *J. Geophys. Res.*, 74, 755, 1969.
- Rycroft, M.J., and J.O. Thomas, The magnetospheric plasmopause and the electron density trough at the Alouette I orbit, presented at the International Symposium on the Physics of the Magnetosphere, Washington, D.C., 1968.
- Serbu, G.P., Results from the IMP-1 Retarding Potential Analyzer, Space Research V, North-Holland Publishing Co., Amsterdam, 1965.
- Serbu, G.P., and E.J.R. Maier, Low Energy Electrons Measured on IMP-2, *J. Geophys. Res.*, 71, 3755-3766, 1966.
- Spitzer, L., Jr., Physics of Fully Ionized Gases, John Wiley & Sons, 1961.
- Taylor, H.A., H.C. Brinton, and C.R. Smith, Positive ion composition in the magneto-ionosphere obtained from the OGO-I satellite, *J. Geophys. Res.*, 70, 5769, 1965.
- Taylor, H.A., Jr., H.C. Brinton, and M.W. Pharo, III, Contraction of the Plasmasphere During Geomagnetically Disturbed Periods, *J. Geophys. Res.*, 73, 961, 1968.
- Trubnikov, B.A., Particle Interactions in a Fully Ionized Plasma, in Review of Plasma Physics, Vol. 1, edited by M.A. Leontovich, 1965.

Whipple, E.C., Jr., The Ion-trap Results in 'Exploration of the Upper Atmosphere with the Help of the Third Soviet Sputnik'," Proc. I.R.E. 47(11):2023-2024, Nov., 1959.

Whipple, E.C. Jr., and L.W. Parker, Theory of an electron trap on a charged spacecraft, J. Geophys. Res., 74, 2962-2971, 1969.

Whipple, E.C. Jr., and L.W. Parker, Effects of secondary electron emission on electron trap measurements in the magnetosphere and solar wind, J. Geophys. Res., 74, 5763-5774, 1969.

OGO-V RETARDING POTENTIAL ANALYZER

SENSOR	ION MODE	FUNCTION
<p>APERTURE</p> <p>RETARDING</p>		<p>a) DEFINE ENTRANCE GEOMETRY</p> <p>b) EXCLUDE ELECTRONS $E < 14\text{eV}$</p>
<p>SUPPRESSOR</p>		<p>a) SUPPRESS SECONDARY ELECTRONS FROM COLLECTOR</p> <p>b) EXCLUDE ELECTRONS $E < 500\text{eV}$</p>
<p>COLLECTOR</p> <p>TO ELECTRONICS</p>		<p>MEASURE CURRENTS IN RANGE: 10^{-12} AMPS $< I_p < 10^{-7}$ AMPS.</p>

Table 1 - Schematic representation of the OGO-V Retarding Potential Analyzer, showing the Sensor grid arrangement and an abbreviated wave-form diagram. All voltages are referenced to spacecraft ground.

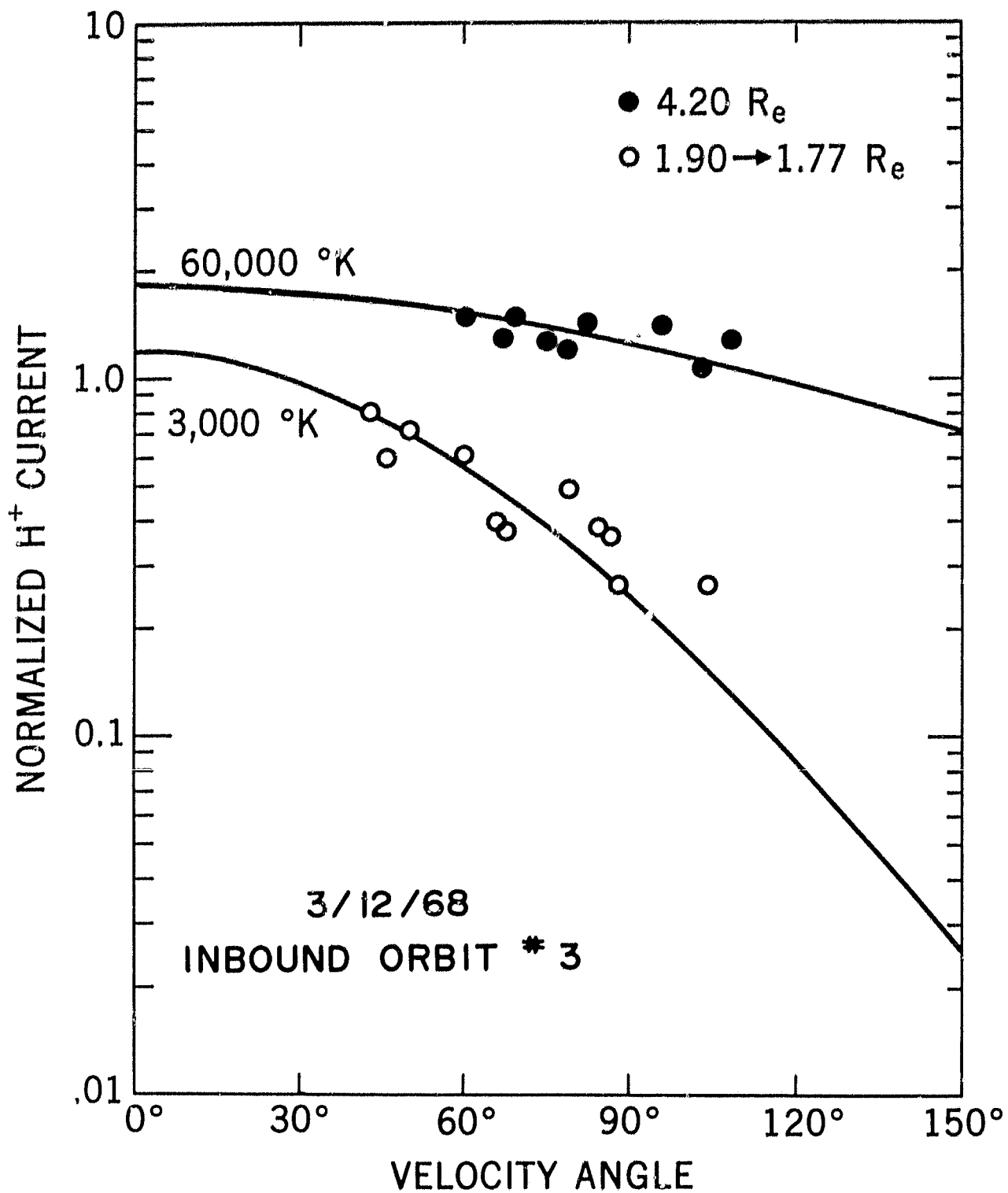


Figure 1 - The data points represent the ion current collected at zero retardations voltage as a function of the angle between the sensor normal and the velocity vector. The smooth curves plotted are the probe response function evaluated as a function of angle for the temperatures indicated. These temperatures were obtained from the computer fits to the complete retardation characteristic sweep range (+15 to -5 volts).

OGO V ION DENSITY

MARCH-APRIL-1968

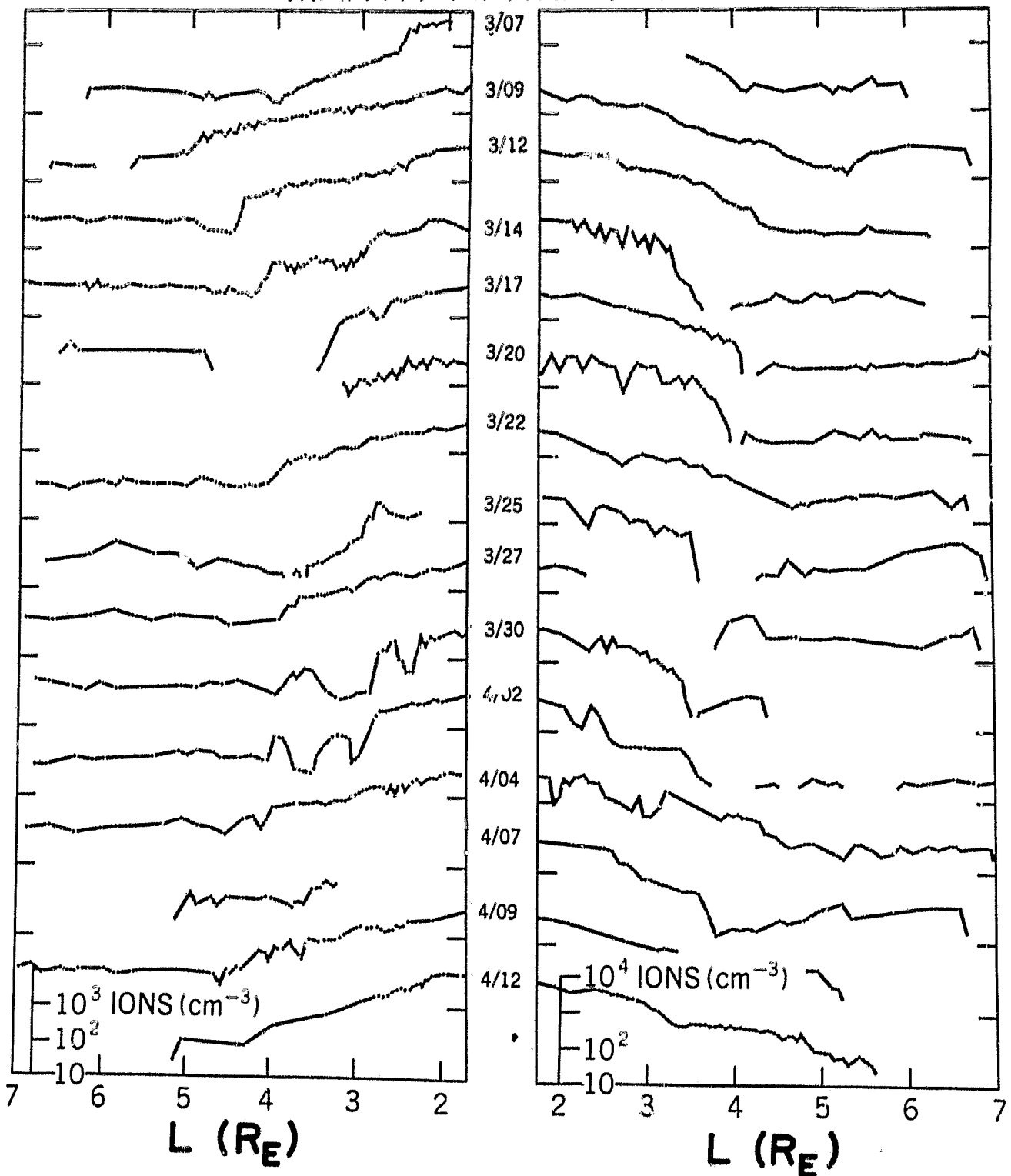


Figure 2 - Observations of Ion Density in the magnetosphere for the first 15 consecutive orbits of OGO-V. The scale shown at the lower left corner slides along the ordinate to the indicated 10^3 level of each curve. The date of perigee is shown in the center, time sequence is from left to right.

OGO V ION TEMPERATURE

MARCH-APRIL - 1968

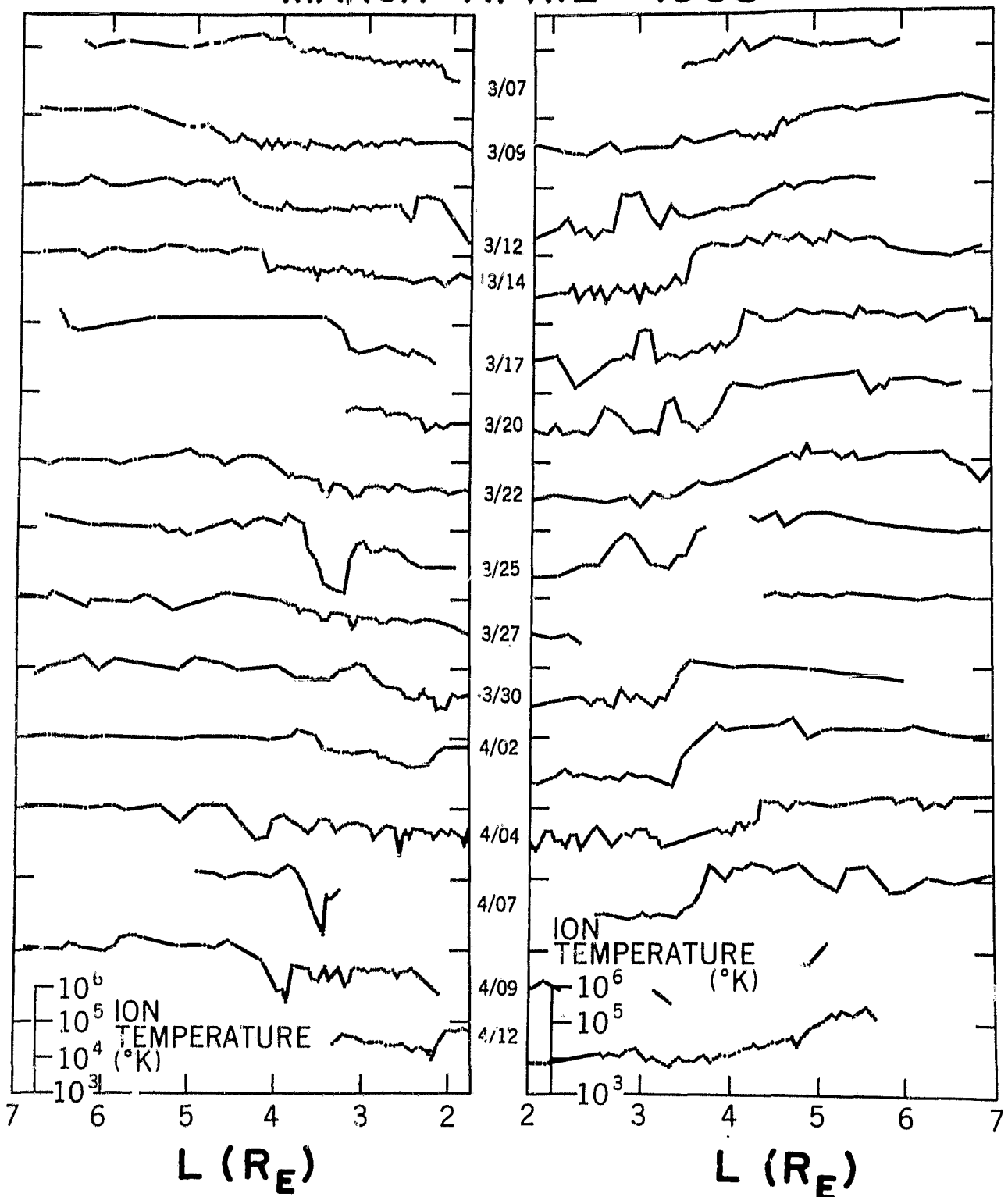


Figure 3 - Observations of ion temperatures in the magnetosphere for the first 15 consecutive orbits of OGO-V. The scale shown at the lower left corner slides along the ordinate to the indicated 10^5 level of each curve.

OGO V PLASMAPAUSE IDENTIFICATION

PERIGEE		±3 HR. AVERAGE			DAYSIDE			NIGHTSIDE		
		DATE 1968	U.T.	K _p	L(R _E)	N _i /N _o	T _o /T _i	L(R _E)	N _i /N _o	T _o /T _i
	3/07	04:25	3-	-	-	-	-	-	-	-
	3/09	18:32	1+	-	-	-	4.6	1	3	-
	3/12	09:18	2+	4.5	10	8	4.0	4	1	-
	3/14	23:46	4	4.3	10	5	3.6	50	12	-
	3/17	14:11	4	3.6	≥ 30	10	4.1	10	20	-
	3/20	04:33	4	-	-	-	4.0	20	25	-
	3/22	18:59	2	4.2	5	3	-	-	-	-
	3/25	09:25	3+	3.6	3	30	3.2	25	14	-
	3/27	23:49	3	3.9	5	1.5	-	-	-	-
	3/30	14:12	5-	2.9	≥ 20	4	3.5	20	14	-
	4/02	04:36	4	3.6	10	3	-	-	-	-
	4/04	19:01	3-	4.1	5	1	4.3	1	4	-
	4/07	09:27	4-	-	-	-	3.8	13	10	-
	4/09	23:53	2	-	-	-	-	-	-	-
	4/12	14:19	2-	-	-	-	-	-	-	-

Table 2 - Tabulation of data used in identifying the location of the plasmopause. The identification is made on the basis of either a jump in the temperature ratio (T_o/T_i) or a jump in the density ratio (N_i/N_o). The dashed lines indicate that identification could not be made on the basis of the data obtained inside L = 7 R_E.

ION TEMPERATURES OGO V
 14 MARCH 1968

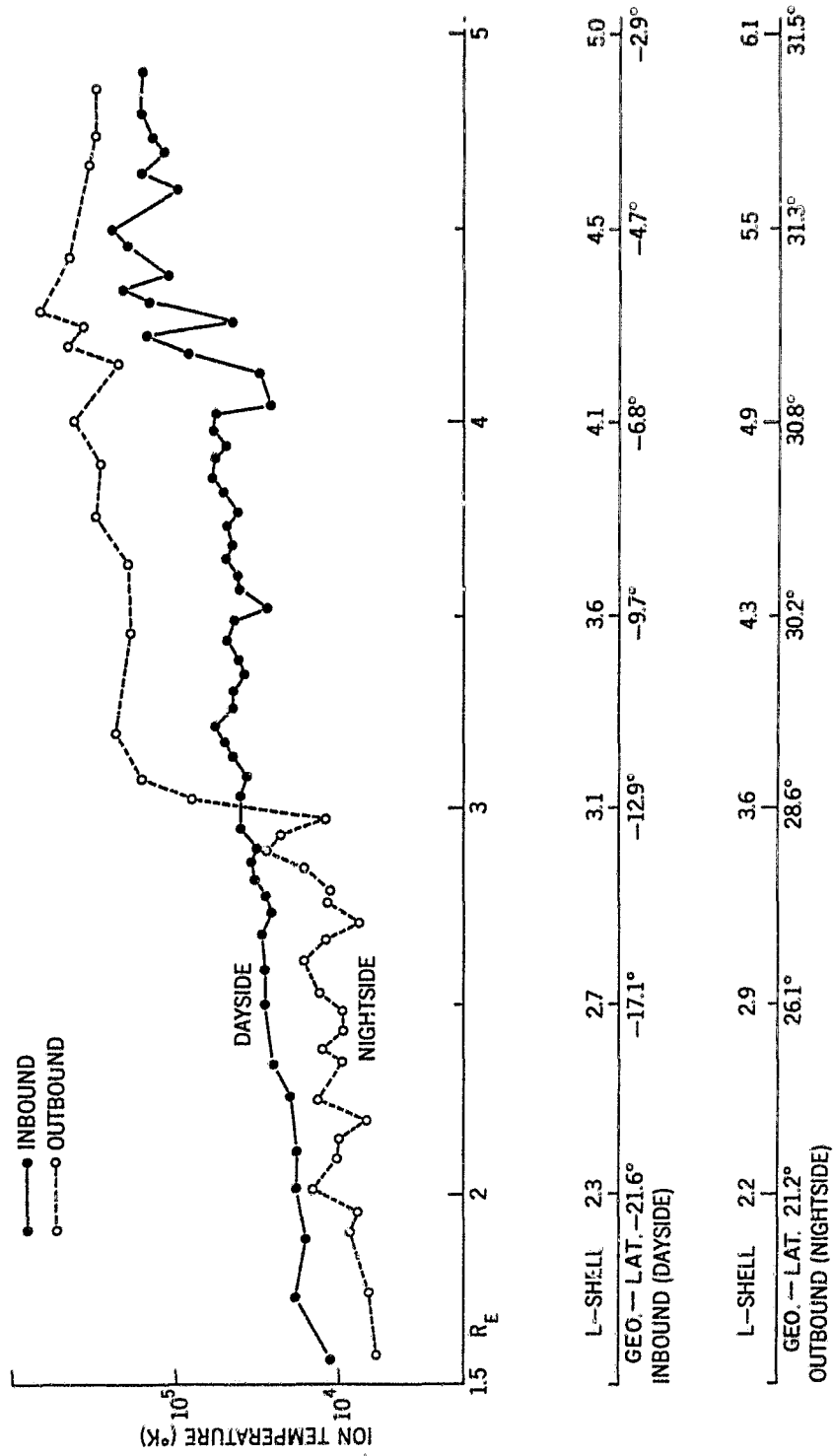


Figure 4 - Detailed temperature profile for the 14th March, 1968 orbital pass. The abscissa is given in terms of Earth radii (R_E) and the L-shell parameters for both inbound and outbound portions of the orbit. The data begins as the spacecraft crosses the geographic equator inbound near $5 R_E$ and terminated some 3 hours later when the spacecraft is outbound at 32° north latitude.

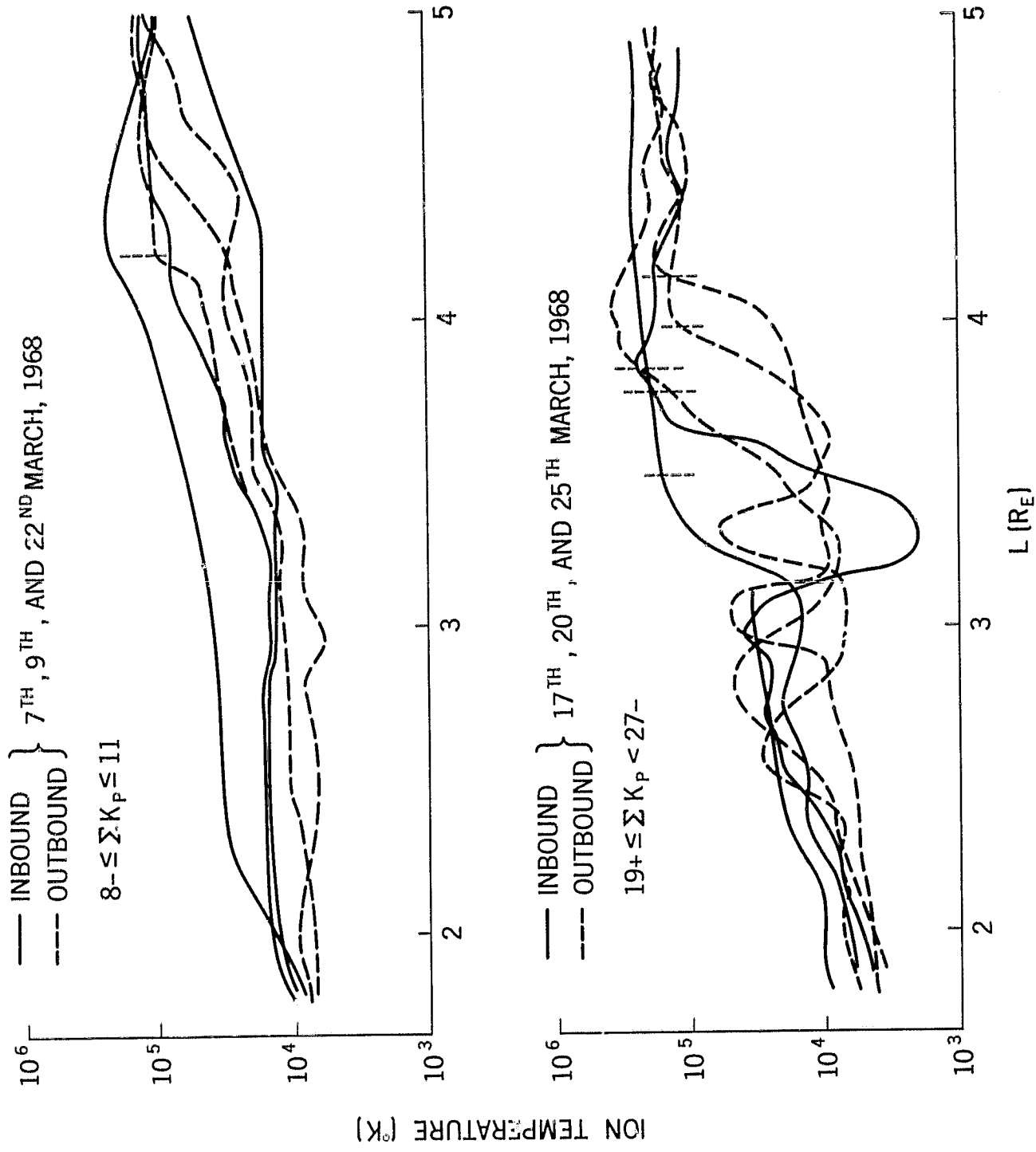


Figure 5 - A series of ion temperature profiles grouped on the basis of the 3 hourly magnetic activity index K_p . The top panel (a) shows the measured profiles for relatively "quiet" times and the lower panel (b) for "disturbed" periods.

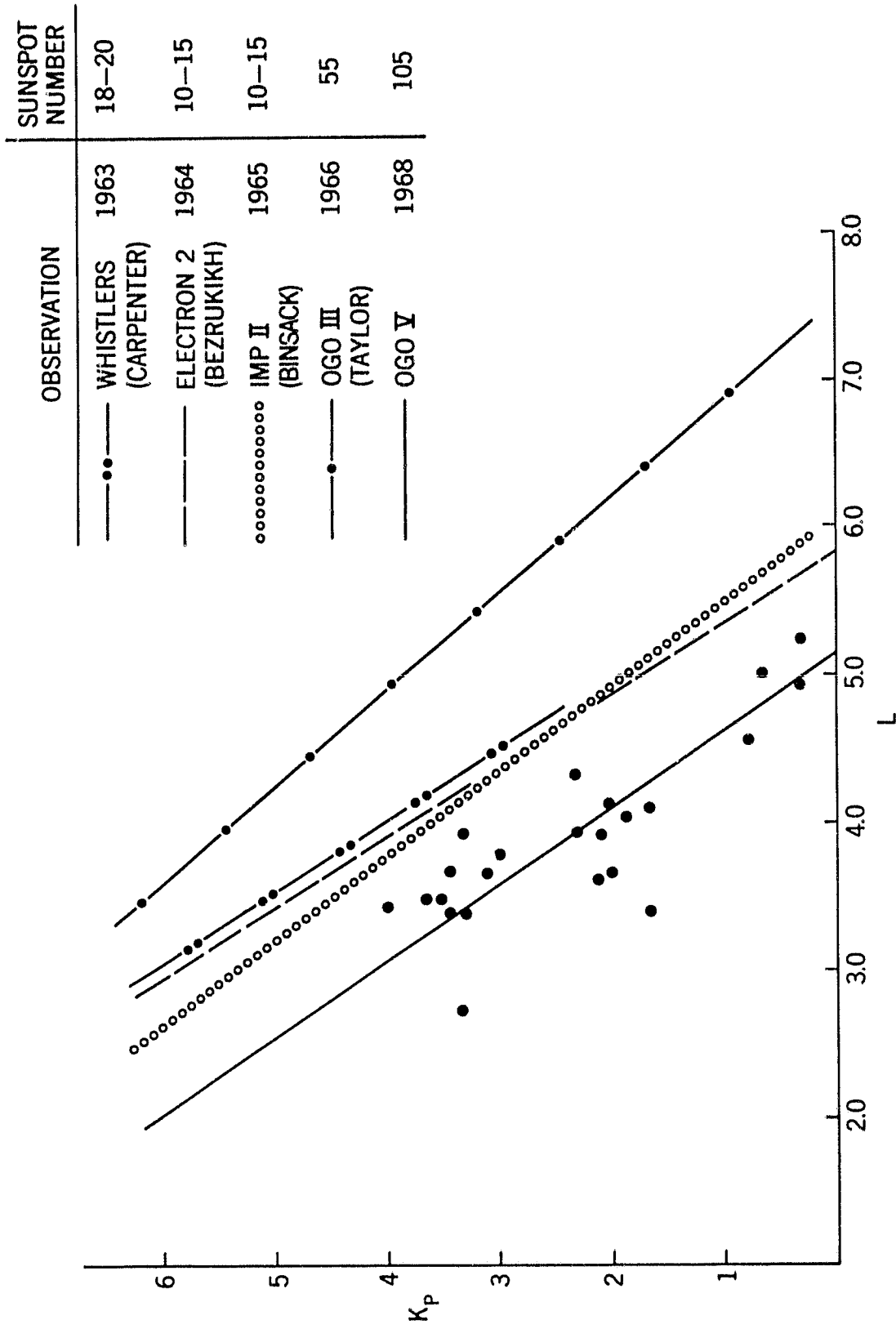


Figure 6 - Data showing the observed radial distance of the plasmopause as a function of the Kp value. A comparison of data obtained over a 5 year period from six spacecrafts is also shown.

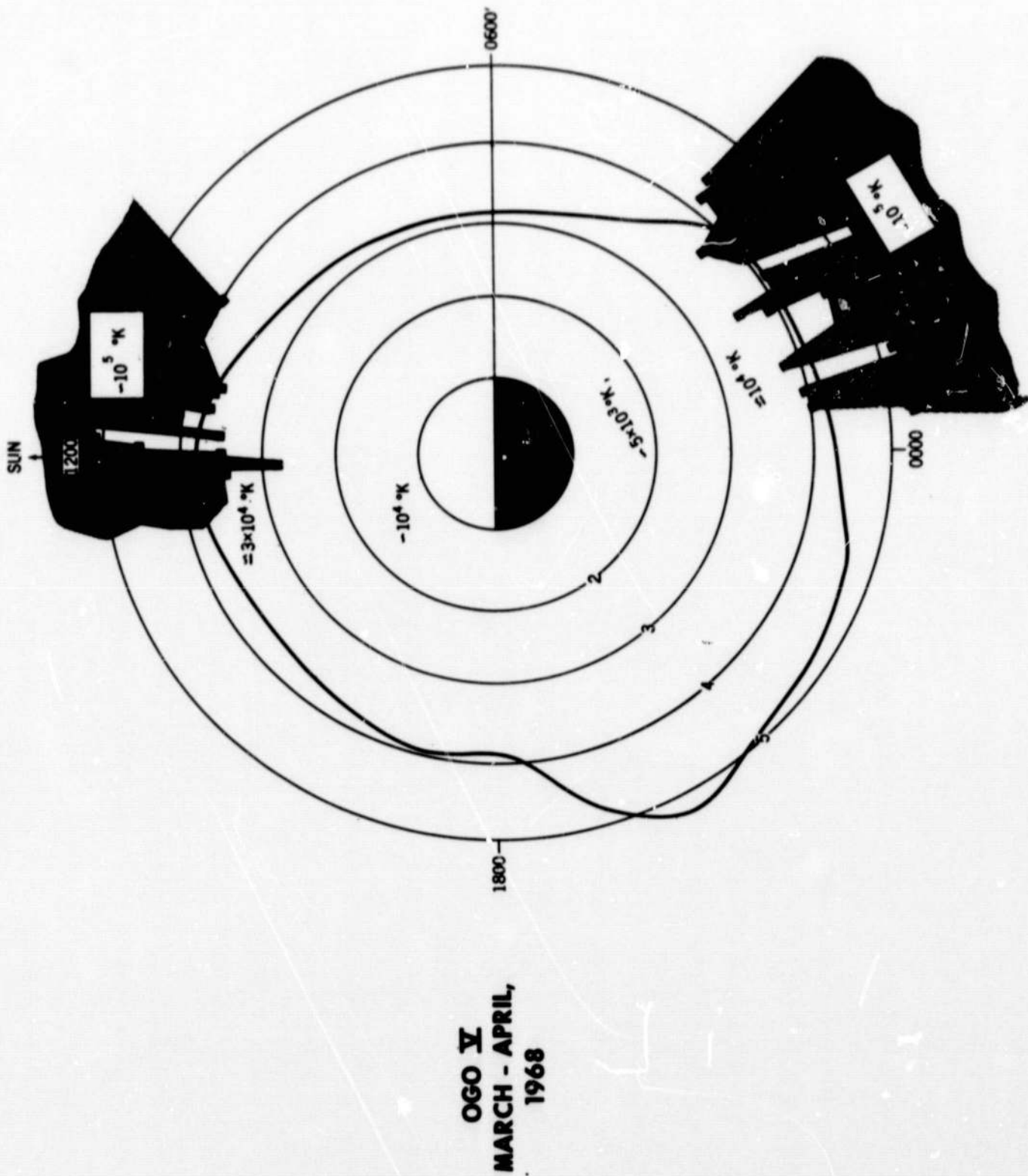


Figure 7 - Projection on the equatorial plane of the plasmapause, as identified on the basis of a thermal discontinuity. The average values of ion temperatures are also indicated.